The $L_{2,3}MM$ Auger electron spectra of solid Ge excited with synchrotron radiation

1994 J. Phys.: Condens. Matter 6 2423

(http://iopscience.iop.org/0953-8984/6/12/017)

J. Phys.: Condens. Matter 6 (1994) 2423–2434. Printed in the UK

The $L_{2,3}MM$ Auger electron spectra of solid Ge excited with synchrotron radiation

Antti Kivimäki
Department of Physics, University of Oulu, FIN-90570 Oulu, Finland

Received 22 November 1993

Abstract. The $L_{2,3}MM$ Auger spectra of solid Ge have been measured using synchrotron radiation excitation. The most intense $L_{2,3}M_{4,5}M_{4,5}$ Auger spectrum has been recorded with several photon energies around the 2p thresholds. As opposed to the 3p thresholds, no core-exciton-induced resonant Auger structures are found. The relative strengths of the different Auger groups have been determined and compared with calculations performed for Ge atoms. The relative intensities of Auger transitions within each Auger group are discussed. Some previously unresolved Auger transitions have been found. The linewidths of Auger transtions are observed to grow when the final-state holes locate in deeper M levels. This final-state broadening implies the presence of Auger cascades.

1. Introduction

Auger electron spectroscopy practised with synchrotron radiation has some advantages compared to more traditional excitation methods such as electron bombardment or Al/Mg Kα x-rays. Provided with the opportunity to select photon energy, one can eliminate some Auger transitions, thus facilitating the interpretation of spectra. This elimination can be applied to adjacent subshells or to unnecessarily deep core levels. The former choice results in the disappearance of the other spin–orbit component in the initial states of Auger transitions while the latter suppresses satellite transitions that occur after the deepest holes have first been filled by Auger processes. This scheme may, of course, be used in the reverse order: the contribution of the satellite transitions can be studied by comparing spectra where they are present and absent.

The LMM Auger spectra of solid Ge were reported earlier by Antonides *et al* [1] and by McGilp and Weightman [2, 3]. Even before that Castle and Epler recorded the photoelectron and Auger spectra of several fourth-period elements [4]. They did not present any detailed analysis on Auger transitions but studied mainly the effects of oxidation. All these investigations were done with Al Kα x-ray radiation (1487 eV). In their study of the $L_{2,3}M_{4,5}M_{4,5}$ Auger groups, McGilp and Weightman [2] also used Mg Kα radiation (1254 eV), just above the L_2 threshold of Ge. They noticed a significant change in the intensity ratio between the $L_3M_{4,5}M_{4,5}$ and $L_2M_{4,5}M_{4,5}$ groups compared to the Al Kα excited spectrum. The effect was supposed to originate from the fall of the L_2 cross section close to the threshold. Our synchrotron radiation excited spectra confirm this conclusion and make it possible to study the changes in the cross section in more detail.

Recently we have studied $M_{2,3}M_{4,5}M_{4,5}$ super-Coster–Kronig transitions in solid Ge and discovered also core-exciton-induced resonant Auger processes around the 3p threshold [5]. When an electron is excited from the 3p shell close to the conduction band minimum,

0953-8984/94/122423+12$19.50

it interacts stongly with the core hole and forms an intermediate bound state. Such a core-excitonic state can decay through Auger emission generating peaks at constant binding energies. This finding motivated us to study whether similar effects could be observed also at the 2p threshold. In the nearby elements Ni and Cu in CuO strong resonances have been reported, but also disputed, at the 2p threshold [6–10]. In those cases, however, the excitation could take place directly to the partly filled 3d band.

2. Experimental details

The Auger spectra of solid Ge have been measured at MAX synchrotron radiation laboratory in Lund, Sweden, using the beamline BL22. The beamline is equipped with a modified SX-700 plane grating monochromator [11]. Of the two gratings supplied, that having 1221 lines mm^{-1} was used in these measurements. Electron spectra were recorded with a Scienta 200 hemisperical analyser [12] combined with an electrostatic electron lens. Pulses were counted with a position-sensitive microchannel plate detector system.

The MAX I storage ring is a low-energy accelerator with a maximum electron energy of 550 MeV. During these measurements the storage ring was operating at 500 MeV. This means a critical energy of about 230 eV when the radius of the bending magnet is 1.2 m [13]. As the 2p binding energies of Ge occur at 1217.0 eV ($2p_{3/2}$) and 1248.1 eV ($2p_{1/2}$) [14], there is a severe lack of intensity at photon energies needed for recording these spectra. The conditions are not so extreme when pure Auger spectra are measured because the exit slits can be set wide open, but if some photon energy resolution is to be maintained the collecting times become disproportionately long. Consequently only moderate electron energy resolution and rather poor photon energy resolution, whenever necessary, could be used in the measurements. The pass energy of the electron analyser was set to 300 or 500 eV, resulting in kinetic energy resolutions of about 1.0 eV and 1.6 eV, respectively. The exit slit size, 200 μm, for the monochromator gives the photon energy resolution of about 6 eV at $h\nu \simeq 1200$ eV.

Two different methods to evaporate a thick Ge film onto substrates were used. A good surface was achieved with Ge pieces squeezed into a spiral tungsten filament. Evaporation was done onto an Au surface, which had earlier been evaporated on a Cu plate. The second time, Ge pieces were put on a boat made of Mo sheet and stainless steel was used as a substrate material. Ge started to vaporize only after the boat was exposed to currents of 32–34 A. This procedure raised the pressure in the preparation chamber considerably and therefore the sample could not be moved immediately to the high vacuum of the analysing chamber. This surface showed carbon contamination so that the intensity of the C 1s signal was $\leqslant 0.3$ of the Ge 3d or 3p when corrected with atomic cross sections given by Yeh and Lindau [15]. No oxygen contamination could be observed. Despite the C contamination on the other surface, both the samples gave similar LMM normal Auger spectra to those published by Antonides *et al* [1] and by McGilp and Weightman [2, 3].

3. Results and discussion

Figure 1(A) shows the $L_{2,3}MM$ Auger spectrum of solid Ge excited with the mean photon energy of 1400 eV. The spectrum was measured using a 500 eV pass energy in the analyser and the opened exit slit of the monochromator. Only the $L_{2,3}M_1M_1$ transitions, which according to multiconfigurational Dirac–Fock (MCDF) calculations have very little intensity,

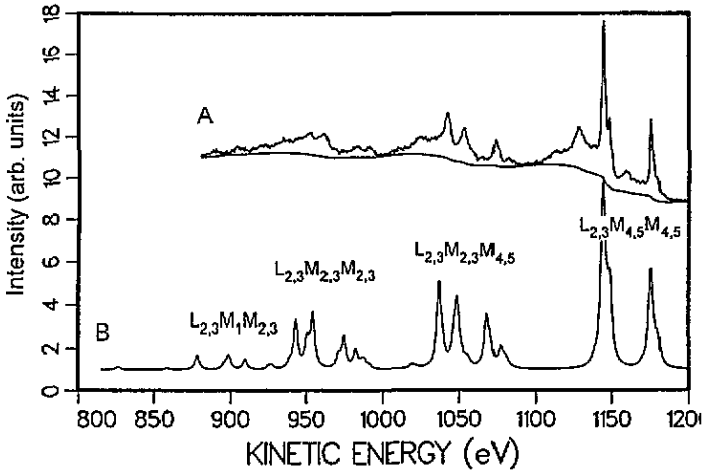

Figure 1. (A) The $L_{2,3}MM$ Auger spectrum of solid Ge measured at $h\nu$=1400 eV. The lower solid curve represents the estimated background. (B) The calculated $L_{2,3}MM$ Auger spectrum of Ge atoms.

fall outside the kinetic energy range of this spectrum. The main Auger groups are labelled in figure 1. Apart from Auger peaks, the spectrum shows also characteristic electron losses due to excitation of plasma oscillations about 16 and 32 eV below the biggest Auger structures.

The lower solid curve in the experimental spectrum of figure 1 estimates the background caused by inelastically scattered electrons. It has been constructed using the 'continuous' background method described in [16] and [17]. The base level of the background is first adjusted at the high-kinetic-energy end of the spectrum. The background at each lower channel is then calculated as a sum from contributions of higher channels multiplied by an exponential attenuation factor. By varying two parameters, the factor before the exponential term and another before the whole summation, the background can be set to match experimental data at a chosen point. This background-subtraction method does not take into account any material-specific phenomena. Thus in the present case the plasmon losses remain in the spectrum. Otherwise the background follows experimental points rather nicely, although the spectrum is very long (320 eV). After the background subtraction peaks can be fitted with symmetrical Voigt functions.

The purpose beyond the background subtraction in the spectrum of figure 1 is to estimate intensity distributions between the different Auger groups and compare them with the calculated profile. As it is not possible to separate all the Auger groups, the measured spectrum has been split only into three parts that roughly correspond to a division: $L_{2,3}M_{2,3}M_{2,3}$ (E_k=880–1000 eV), $L_{2,3}M_{2,3}M_{4,5}$ (E_k=1000–1095 eV) and $L_{2,3}M_{4,5}M_{4,5}$ (E_k=1100–1190 eV). The intensity in the given kinetic energy ranges has simply been integrated. The plasmon structures have also been included in the total intensity, because they cannot be taken away reliably. Since the plasmons acquire their intensity from the Auger peaks, this inclusion is conceptually not so wrong, inasmuch as they belong to the same part as their generator lines. The spectrum has not been transmission corrected. The transmission function of the analyser is not known but it is probably almost constant at such high kinetic energies. For all these uncertainties the extracted values listed in table 1 are only qualitative.

The Auger transitions in question occur between the core levels. Therefore all the holes are localized to the same atom and an atomic approach for the Auger processes should be

Table 1. Experimental and calculated intensity distributions between $L_{2,3}MM$ Auger groups. Calculated energies are also given.

Auger group	Experimental intensity (%)	Calculated intensity (%)		Calculated energies (eV)
$L_3M_1M_1$	—	0.31		812.4
$L_2M_1M_1$	—	0.16		843.8
$L_3M_1M_{2,3}$	22	3.36	26.2	863.9–884.9
$L_2M_1M_{2,3}$		1.68		895.3–916.0
$L_3M_{2,3}M_{2,3}$		13.31		925.1–940.1
$L_2M_{2,3}M_{2,3}$		6.66		956.5–971.5
$L_3M_1M_{4,5}$		1.17		973.4–976.9
$L_2M_1M_{4,5}$	27	0.59	30.8	1004.8–1008.3
$L_3M_{2,3}M_{4,5}$		20.26		1022.5–1043.0
$L_2M_{2,3}M_{4,5}$		9.90		1053.9–1074.3
$L_3M_{4,5}M_{4,5}$	51	28.77	42.6	1124.2–1134.9
$L_2M_{4,5}M_{4,5}$		13.83		1155.6–1166.3

adequate. Actually, the $L_{2,3}M_{4,5}M_{4,5}$ Auger spectrum of atomic Ge has been published [18] and it is very similar to that from the solid-state phase. The atomic calculations presented so far are non-relativistic [1–3] or restricted to the $L_{2,3}M_{4,5}M_{4,5}$ transitions [18]. In this work, the energies and intensities of all possible $2p^{-1} \rightarrow (3s3p3d)^{-2}$ Auger transitions have been calculated for Ge atoms. The energies were obtained from the MCDF code of Grant *et al* [19] and transition probabilities were computed using the method described in [20]. The ground state of Ge was supposed to be $[Ar]3d^{10}4s^24p_{1/2}^2$, which is a closed-shell electron configuration in the applied jj coupling scheme ([Ar] stands for the electron configuration of Ar). We shall denote final states using LS-symbols but it should be remembered that they are not pure LS-states.

The calculated profile shown in figure 1 was constructed using 3.2 eV broad Lorentzian lines, which seem to be too wide for the $L_{2,3}M_{4,5}M_{4,5}$ Auger transitions and too narrow for the transitions in the low-kinetic-energy end of the spectrum. Further considerations about the linewidths will be presented later. The calculated spectrum of figure 1 has been shifted by about 15 eV to higher kinetic energies to coincide better with experiment. The experimental free-atom–solid Auger energy shift has been reported to be 18.7 eV [18]. In the case of the $L_{2,3}M_{4,5}M_{4,5}$ Auger processes, the difference between our calculated energies and the measured kinetic energies in Ge atoms is smaller than 4 eV [18]. The calculated intensities and energies for the Auger groups are displayed in table 1. As can be seen from both the experimental and theoretical results, the $L_{2,3}M_{4,5}M_{4,5}$ Auger lines dominate but the contributions of the other groups cannot be neglected by any means. We shall shortly study each part of the spectrum in more detail.

The final-state holes can, of course, locate also in the valence (N) shell but the simultaneous calculation of these transitions was hindered by the orthogonality problems between the 3p and 4p wave functions. The intensity of the Auger transitions, where one or both of the final-state holes are in the N shell, is probably very weak. McGilp and Weightman [2] interpreted one broad plateau-like feature in their spectrum as an $L_3M_{4,5}N_{2,3}$ structure. This same feature can indeed be seen in the experimental spectrum of figure 1 as a small shoulder just above the $L_2M_{4,5}M_{4,5}$ Auger lines.

3.1. $L_{2,3}M_{4,5}M_{4,5}$ Auger processes

Figure 2 shows some of the $L_{2,3}M_{4,5}M_{4,5}$ Auger spectra recorded with different photon

energies around the $L_{2,3}$ thresholds. These spectra were measured with a 300 eV pass energy for the analyser and a 200 μm exit slit in the monochromator, except for the 1400 eV spectrum, which was measured with opened slits. In these experimental conditions the strongest Auger peaks, $L_{2,3}M_{4,5}M_{4,5}$ ($^1G_4$) had halfwidths of 1.6–1.7 eV. The 3d photoelectron line, seen in the lowest spectrum at E_k=1173 eV, was typically 6.5–7.0 eV wide, most of which originates from the bandwidth of the photon beam. All structures in the spectra can be assigned to non-resonant Auger lines, photoelectron lines or plasmon losses. The apparent changes at the low-kinetic-energy side of the spectra at $h\nu$=1249 and 1258 eV are explained by the 3p photoelectron lines that crawl into the region. No sign of core-exciton-induced resonant Auger processes can be observed. They cannot, however, be excluded completely because of poor photon energy resolution.

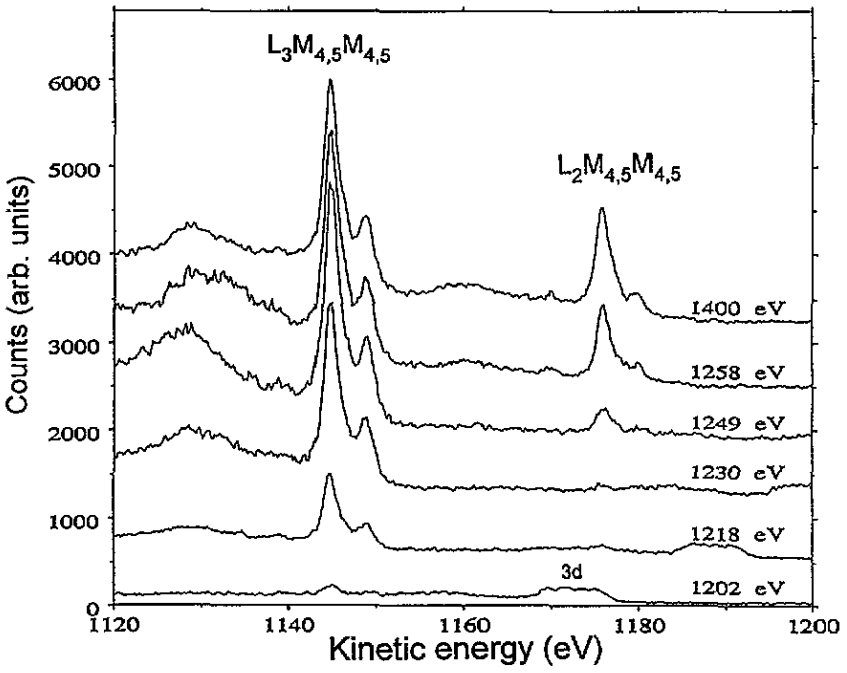

Figure 2. The $L_{2,3}M_{4,5}M_{4,5}$ Auger spectrum measured at different photon energies around the 2p thresholds.

The lowest spectrum of figure 2 is measured at $h\nu$=1202 eV, which is well below the L_3 threshold of 1217.0 eV [14]. Despite this, some $L_3M_{4,5}M_{4,5}$ Auger structure is visible. It probably originates from stray light that passes the monochromator without being monochromatized when the grating is working in extremely small grazing angles. The second-order light contribution should be practically non-existent. When the photon energy increases the $L_3M_{4,5}M_{4,5}$ Auger group grows gradually until about 30 eV above the threshold. Here we have compared the intensity to the 3d photoline, which is of course not a reliable reference because the cross section of the 3d changes also as a function of photon energy. The $L_2M_{4,5}M_{4,5}$ Auger structure starts to grow when the L_2 threshold is crossed. The same gradual increment can be observed as in the case of the $L_3M_{4,5}M_{4,5}$ Auger transitions. The $L_3M_{4,5}M_{4,5}/L_2M_{4,5}M_{4,5}$ intensity ratio calculated from the sum

intensities of individual Auger peaks decreases from about 6.1 at 1249 eV to 3.4 at 1258 eV and to 2.05 at 1400 eV. This last result agrees well with the statistical population ratio of two between the L_3 and L_2 subshells. The MCDF calculations performed predict a ratio of 2.08 between the $L_3M_{4,5}M_{4,5}$ and $L_2M_{4,5}M_{4,5}$ Auger line intensities. The experimental intensity ratio was obtained after using the background subtraction described in the previous chapter. The fit of the spectrum is displayed in figure 3. A different background affected the intensity ratio surprisingly little, as a Shirley background estimation gave only a slightly smaller intensity ratio of 2.01. From the Al Kα excited Auger spectra the intensity ratio was earlier reported to be 2.3 by McGilp and Weightman [2]. The small discrepancy could perhaps be explained by their apparent omission of the two-bulk plasmon loss peak that accompanies the $L_2M_{4,5}M_{4,5}$ Auger structure and lies just under the $L_3M_{4,5}M_{4,5}$ Auger group. The $L_2L_3M_{4,5}$ Coster–Kronig processes are energetically impossible in Ge, which is born out just in the fact that the intensity ratio draws near to the statistical weight. The case is different in Cu and Zn, where the observed intensity ratio between the $L_3M_{4,5}M_{4,5}$ and $L_2M_{4,5}M_{4,5}$ Auger groups is strongly distorted [1, 21].

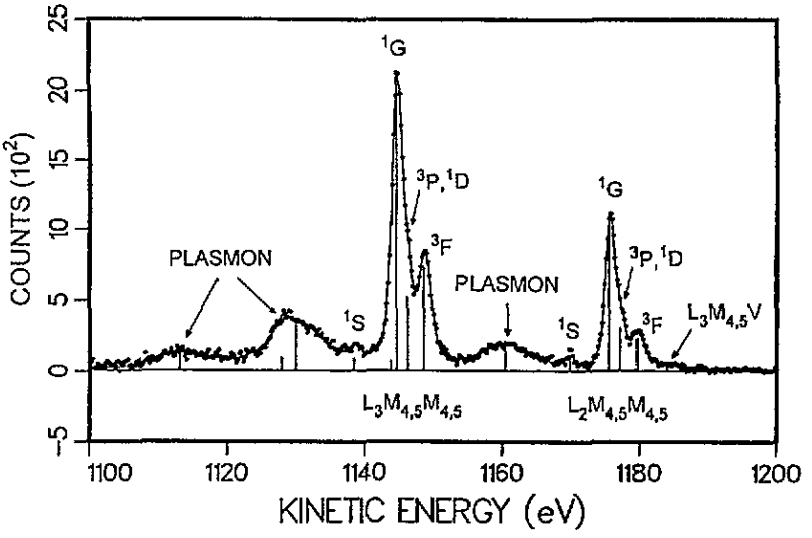

Figure 3. The background-subtracted $L_{2,3}M_{4,5}M_{4,5}$ Auger spectrum recorded at the mean photon energy of 1400 eV. The vertical bars indicate the positions of the peaks. An assignment for the peaks is given. The solid curve represents the fit.

The relative intensities of the Auger transitions within the same group are more sensitive to the chosen background than the total intensity ratio between the two Auger groups. The experimental values shown in table 2 are derived from the fit of figure 3. Theoretical relative intensities are also presented in table 2. Both experiment and theory give about 60% of the total intensity to the $^1G_4$ terms. From figure 3 it is evident that the ^3F term has proportionally more intensity in the $L_3M_{4,5}M_{4,5}$ group than in the $L_2M_{4,5}M_{4,5}$ group. Here theory agrees almost perfectly with the values obtained from the fit. The ^3P and ^1D terms on the high-kinetic-energy side of the ^1G peak could not be resolved. In the fitting only one peak was placed there. Table 2 shows its intensity as if it were the sum of ^3P and ^1D. The ^3P term could have been combined equally well with ^1G because the calculated term splitting is only slightly bigger then. Thus the experimental intensity distribution between

^{1}G, ^{3}P and ^{1}D is only indicative. The same applies also to the kinetic energy of the joint ^{3}P–^{1}D peak. The energies shown in table 2 agree quite well with those given by Antonides *et al* [1]. The relative energies of McGilp and Weightman [2] are probably the most accurate but they used the vacuum level as a reference instead of the top of the valence band.

Table 2. Kinetic energies of the $L_{2,3}M_{4,5}M_{4,5}$ Auger transitions relative to the top of the valence band. Experimental and calculated relative intensities are also given.

Auger process	Term	Experimental energy (eV)	Experimental intensity (%)	Calculated intensity (%)
$L_3M_{4,5}M_{4,5}$	^{1}S	1138.9±0.3	2	2.1
	^{1}G	1144.9±0.1	55	59.4
	^{3}P	1146.5±0.3	15	4.1
	^{1}D			6.8
	^{3}F	1149.0±0.1	28	27.6
$L_2M_{4,5}M_{4,5}$	^{1}S	1170.1±0.2	5	2.6
	^{1}G	1176.0±0.1	59	63.1
	^{3}P	1177.5±0.3	17	6.8
	^{1}D			9.7
	^{3}F	1180.0±0.2	18	17.9
$L_3M_{4,5}V$	—	1184±3	—	—

3.2. $L_{2,3}M_{2,3}M_{4,5}$ *Auger processes*

As the $L_{2,3}M_{4,5}M_{4,5}$ Auger spectra did not reveal any peculiarities at the $L_{2,3}$ thresholds, the $L_{2,3}M_{2,3}M_{4,5}$ spectra were recorded only with few photon energies. Here synchrotron radiation does not provide much new information, because the transitions do not overlap. The assignment presented in [1] is correct.

We can demonstrate the disappearance of the L_2-based Auger transitions when the photon energy is set between the L_2 and L_3 thresholds. In that case the 3s photoelectron line occurs at the same kinetic energies as the $L_3M_{2,3}M_{4,5}$ Auger structure. To estimate its contribution the spectra were measured with photon energies of about 1228 and 1238 eV. Peak heights were only marginally different, hence the spectra were added. The result shown in figure 4(A) was obtained after subtracting the 'continuous' background from the sum. The spectrum of figure 4(B) is a sum of the $L_{2,3}M_{2,3}M_{4,5}$ measurements after a similar background subtraction. The shape of the original spectrum can been seen in figure 1.

The $L_{2,3}M_{2,3}M_{4,5}$ Auger spectrum is too complicated for unambiguous interpretation. The following *LS*-terms in order of increasing kinetic energy are possible for $3p^{-1}3d^{-1}$ final states: ^{1}F, ^{1}P, ^{3}D, ^{3}P, ^{1}D and ^{3}F. Furthermore, according to MCDF calculations the triplets are spread to 1.1–2.8 eV wide regions. Anyway, it is obvious that the low-kinetic-energy peak in both Auger groups is composed mainly of the ^{1}F term and to a lesser extent of the ^{1}P term. The high-energy peaks arise from the ^{3}D and ^{3}P terms. Theory predicts nicely the diminution of this peak in the $L_2M_{2,3}M_{4,5}$ Auger group as can seen from figure 1 and from the calculated intensities shown in table 3. The shoulder on the high-kinetic-energy side of the second peak in the $L_3M_{2,3}M_{4,5}$ Auger group probably originates from the ^{1}D

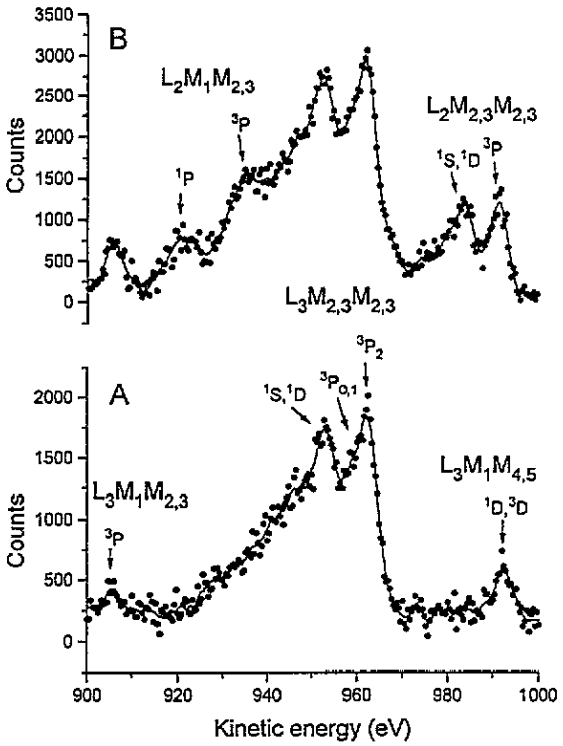

Figure 4. The $L_{2,3}M_{2,3}M_{4,5}$ Auger spectrum measured between the L_2 and L_3 thresholds (A) and above both the thresholds (B).

and ^3F terms. It appears in all of our spectra and should therefore be an integral part of the $L_3M_{2,3}M_{4,5}$ Auger decay, thus confirming the speculations of McGilp and Weightman [3] about its origin. The spectrum of figure 4(A) conclusively removes the possibility that this shoulder could be a plasmon loss peak. The experimental energies for the $L_{2,3}M_{2,3}M_{4,5}$ Auger transitions are also given in table 3. It can be noted that the energy difference between the high-kinetic-energy peaks of the two Auger groups is clearly smaller than the L_2–L_3 spin–orbit splitting of 31.1 ± 0.1 eV, which is in accordance with the decrease of the higher-energy term ^3P as predicted by the MCDF calculations. It starts to seem as if theoretical relative intensities are quite close to reality.

Apart from the $L_{2,3}M_{2,3}M_{4,5}$ Auger transitions, the $L_2M_1M_{4,5}$ Auger processes should also locate in this kinetic energy range. No distinct peaks can be observed immediately, but if the spectra of figure 4 are examined on top of each other, the plasmon structure below the $L_3M_{2,3}M_{4,5}$ Auger group is seen to change its shape. This small peak could be mainly due to the $L_2M_1M_{4,5}$ (^1D) transition because theory gives much lower intensity for the ^3D term. The location of the extracted peak agrees with the sum of the kinetic energy of the corresponding peak in the $L_3M_1M_{4,5}$ Auger group, which is clearly discerned in figure 5, and the L_2–L_3 spin–orbit splitting.

3.3. $L_{2,3}M_{2,3}M_{2,3}$ and $L_{2,3}M_1M_{2,3}$ Auger processes

Figure 5 shows the kinetic energy region 900–1000 eV measured with photon energies between the $L_{2,3}$ thresholds (A) and above the thresholds (B). The 'continuous' background

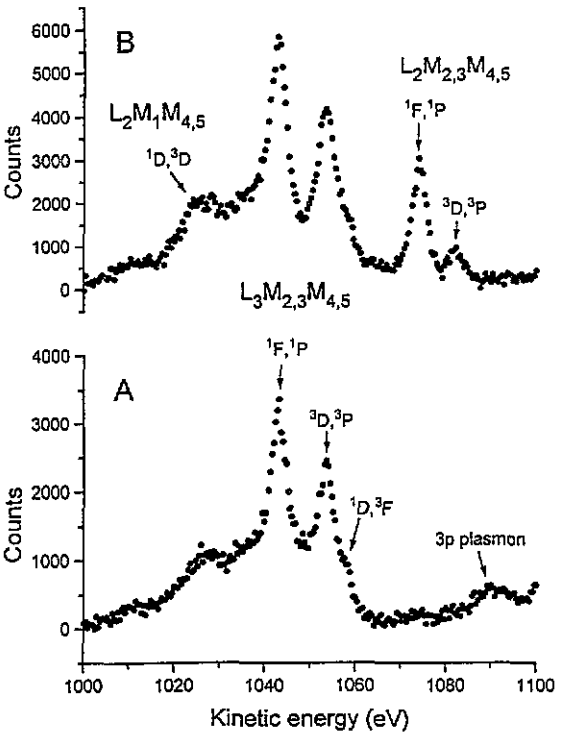

Figure 5. The $L_{2,3}M_{2,3}M_{2,3}$ and $L_{2,3}M_1M_{2,3}$ Auger spectra measured between the L_2 and L_3 thresholds (A) and above both the thresholds (B). The solid line shows smoothed data.

has been subtracted from the spectra, even though its effect is now rather small. The kinetic energies and calculated relative intensities for all the transitions of this region are presented in table 4. Also the $L_3M_1M_{2,3}$ (^1P) peak seen only in figure 1 is included.

The strongest structures in the spectra are caused by the $L_{2,3}M_{2,3}M_{2,3}$ Auger transitions. The possible *LS*-terms are ^1S, ^1D and ^3P. Calculations split the ^3P levels into two peaks, since the energy difference between the two lowest components, $^3P_0$ and $^3P_1$ is only 0.6 eV whereas $^3P_2$ locates 3.2 eV higher than $^3P_1$. The effect can be observed also in the experimental data where the higher peak of the $L_3M_{2,3}M_{2,3}$ structure has a clear shoulder on the low-kinetic-energy side. Theory gives interestingly most intensity to the $^3P_2$ component (see table 4) in the $L_3M_{2,3}M_{2,3}$ Auger group, but in the $L_2M_{2,3}M_{2,3}$ group it has only 6.3% of the total intensity, being the second weakest transition. Unfortunately this problem cannot be clarified from the measured spectrum. The statistics are too poor and the $L_3M_1M_{4,5}$ Auger structure can be seen to coincide with the $L_2M_{2,3}M_{2,3}$ (^3P) peak.

3.4. Linewidths of Auger transitions

The poor resolution of these spectra is not solely due to the spectrometer, but the Auger peaks are also broadened by the further decay of the final states. For instance, the final states $3p^{-2}$ produced by the $L_{2,3}M_{2,3}M_{2,3}$ Auger processes can decay, e.g., to $3p^{-1}3d^{-2}$ states. Because of the lack of isolated and intense Auger lines it is not possible to give accurate values for how much Auger peaks are broadened when final-state holes of the diagram Auger transitions locate in increasingly deeper shells. Therefore the numbers to be

Table 3. Calculated relative intensities and kinetic energies of the $L_{2,3}M_{2,3}M_{4,5}$ Auger transitions relative to the top of the valence band.

Auger process	Term	Experimental energy (eV)	Calculated intensity (%)
$L_2M_1M_{4,5}$	^1D	1024 ± 2	72.3
	^3D		27.7
$L_3M_{2,3}M_{4,5}$	^1F	1043.3 ± 0.3	39.7
	^1P		8.4
	^3D	1053.7 ± 0.3	29.7
	^3P		15.2
	^1D	1058.4 ± 0.5	2.6
	^3F		4.4
$L_2M_{2,3}M_{4,5}$	^1F	1074.3 ± 0.3	47.6
	^1P		21.2
	^3D	1082.5 ± 0.3	25.0
	^3P		5.3
	^1D	—	0.6
	^3F	—	0.4

Table 4. Calculated relative intensities and kinetic energies of the $L_{2,3}M_1M_{2,3}$ and $L_{2,3}M_{2,3}M_{2,3}$ Auger transitions relative to the top of the valence band.

Auger process	Term	Experimental energy	Calculated intensity (%)
$L_3M_1M_{2,3}$	^1P	890±2 eV	44.2
	^3P	906±2 eV	55.8
$L_2M_1M_{2,3}$	^1P	921±2 eV	60.8
	^3P	935±2 eV	39.2
$L_3M_{2,3}M_{2,3}$	^1S	953.4±1.0 eV	4.5
	^1D		35.6
	$^3P_{0,1}$	958.7±1.0 eV	21.3
	$^3P_2$	962.6±0.5 eV	38.6
$L_2M_{2,3}M_{2,3}$	^1S	983.9±1.0 eV	19.5
	^1D		46.6
	^3P	991±2 eV	33.9
$L_3M_1M_{4,5}$	^1D	992.5±1.0 eV	69.8
	^3D		30.2

presented are far from quantitative. The final-state broadening can be estimated from the analytical expression

$$\frac{\Gamma_L}{\Gamma_{tot}} = 1 - \left(\frac{\Gamma_G}{\Gamma_{tot}}\right)^2 - 0.114\left(1 - \frac{\Gamma_G}{\Gamma_{tot}}\right)\left(\frac{\Gamma_G}{\Gamma_{tot}}\right)^2$$

given in [22]. Here Γ_G is the Gaussian contribution describing the intrumental broadening and Γ_L is the Lorentzian contribution representing the arithmetic sum of the initial- and final-state widths.

As already mentioned the $L_{2,3}M_{4,5}M_{4,5}$ (^1G) peaks have total linewidths of 1.6–1.7 eV. The analyser is estimated to cause a Gaussian broadening of about 1.0 eV at a 300 eV pass energy. If the $L_{2,3}$ core holes have an inherent broadening of the order of 1.0 eV [23] then the above formula gives the broadening of only 0.0–0.1 eV for the $3d^{-2}$ states. This result means a long-lived state and points out that further Auger decay is improbable or even impossible. The almost pure $L_3M_{2,3}M_{4,5}$ (^1F) peak in figure 4 has a total linewidth of about 4.5 eV. Using now a 1.6 eV Gaussian line for the instrumental broadening at 500 eV pass energy, the width of 2.9 eV can be calculated for the $3p^{-1}3d^{-1}$ final states. The fit of the $L_{2,3}M_1M_{2,3}$ (^1P) singlets yields widths of 5–6 eV. The choice of the mid-value 5.5 eV results in a lifetime broadening of 4.0 eV for the $3s^{-1}3p^{-1}$ configuration.

These results can be compared with the widths of the single-hole states obtained from the photoelectron lines. Yin *et al* have reported the widths of 2.0 ± 0.2 eV and 2.1 ± 0.2 eV for the 3s and $3p_{1/2,3/2}$ photolines in solid Ge, respectively [24]. The Ge 3d photoelectron lines have recently been extensively studied as it has become possible to distinguish the contributions arising from bulk and surface atoms [25, 26]. The inherent broadening of the 3d is obviously about 0.3 eV. Thus in the case of the $3d^{-2}$ final states the lifetime broadening becomes smaller than in the corresponding single-hole state $3d^{-1}$. All the other hole combinations seem to lead to final states that have shorter lifetimes than the related single-M-hole states. The absence of final-state broadening certainly makes the Ge $L_3M_{4,5}M_{4,5}$ Auger transitions good candidates in searching for bulk–surface shifts in Auger spectra.

3.5. Conclusions

The $L_{2,3}$-based Auger transitions have been studied using synchrotron radiation. The experimental spectrum has been compared with a theoretical profile obtained from MCDF calculations for Ge atoms. Theory has been seen to reproduce the Auger spectrum surprisingly well. Of the several possible Auger processes, the $L_{2,3}M_{4,5}M_{4,5}$ transitions are most intense, but the $L_{2,3}M_{2,3}M_{4,5}$ and $L_{2,3}M_{2,3}M_{2,3}$ Auger groups are also quite strong. The intensity ratio between the $L_3M_{4,5}M_{4,5}$ and $L_2M_{4,5}M_{4,5}$ Auger transitions has been found to be 2.05 ± 0.1, in close accordance with the statistical weight between the L_3 and L_2 subshells and also with the MCDF calculations. The Auger structures were observed to grow gradually upto about 30 eV above the threshold, reflecting the behaviour of the $L_{2,3}$ cross sections. Some previously unresolved Auger lines, notably those having one of the final-state holes in the 3s orbital, have been uncovered. The widths of the Auger peaks have been observed to broaden when the final hole states locate in the deeper shells, indicating the effects of the Auger cascades.

Acknowledgments

The author is grateful to Professor Seppo Aksela and Dr Helena Aksela for stimulating discussions and critical reading of the manuscript. Dr Olli-Pekka Sairanen is acknowledged for cooperation during the measurements and Dr Ergo Nõmmiste for preparation of the

sample. The staff of MAX Laboratory are thanked for assistance. The author would like to acknowledge the financial support from the Research Council for the Natural Sciences of the Academy of Finland.

References

[1] Antonides E, Janse E C and Sawatzky G A 1977 *Phys. Rev.* B **15** 1669, 4596
[2] McGilp J F and Weightman P 1976 *J. Phys. C: Solid State Phys.* **9** 3451
[3] McGilp J F and Weightman P 1978 *J. Phys. C: Solid State Phys.* **11** 643
[4] Castle J E and Epler D 1974 *Proc. R. Soc.* A **339** 49
[5] Kivimäki A, Aksela H, Aksela S and Sairanen O-P 1993 *Phys. Rev.* B **47** 4181
[6] Tjeng L H, Chen C T, Ghijsen J, Rudolf P and Sette F 1991 *Phys. Rev. Lett.* **67** 501
[7] van der Laan G, Surman M, Hoyland M A, Flipse C F J, Thole B T, Seino Y, Ogasawara H and Kotani A 1992 *Phys. Rev.* B **46** 9336
[8] López M F, Höhr A, Laubschat C, Domke M and Kaindl G 1992 *Europhys. Lett.* **20** 357
[9] Tjeng L H 1993 *Europhys. Lett.* **23** 535
[10] López M F, Laubschat C and Kaindl G 1993 *Europhys. Lett.* **23** 538
[11] Nyholm R, Svensson S, Nordgren J and Flodström A 1986 *Nucl. Instrum. Methods* A **246** 267
[12] Andersen J N, Björneholm O, Sandell A, Nyholm R, Forsell J, Thånell L, Nilsson A and Mårtensson N 1991 *Synchrot. Radiat. News* **4** 15
[13] Eriksson M 1982 *Nucl. Instrum. Methods* **196** 331
[14] Ley L and Cardona M (ed) 1979 *Photoemission in Solids II* (Berlin: Springer)
[15] Yeh J J and Lindau I 1985 *At. Data Nucl. Data Tables* **32**
[16] Aksela H, Väyrynen J and Aksela S 1979 *J. Electron Spectrosc. Relat. Phenom.* **16** 339
[17] Chorkendorff Ib, Onsgaard J, Aksela H and Aksela S 1983 *Phys. Rev.* B **27** 945
[18] Aksela S and Aksela H 1985 *Phys. Rev.* A **31** 1540
[19] Grant I P, McKenzie B J, Norrington P H, Mayers D F and Pyper N C 1980 *Comput. Phys. Commun.* **21** 207, 233
[20] Aksela H, Aksela S, Tulkki J, Åberg T, Bancroft G M and Tan K H 1989 *Phys. Rev.* A **39** 3401
[21] Wassdahl N, Rubensson J-E, Bray G, Glans P, Bleckert P, Nyholm R, Cramm S, Mårtensson N and Nordgren J 1990 *Phys. Rev. Lett.* **64** 2807, and references therein
[22] Keski-Rahkonen O and Krause M O 1977 *Phys. Rev.* A **15** 959
[23] Weightman P, McGilp J F and Johnson C E 1976 *J. Phys. C: Solid State Phys.* **9** L585
[24] Yin L I, Adler I, Tsang T, Chen M H, Ringers D A and Crasemann B 1974 *Phys. Rev.* A **9** 1070
[25] Le Lay G, Kanski J, Nilsson P O, Karlsson U O and Hricovini K 1992 *Phys. Rev.* B **45** 6692
[26] Cao R, Yang X, Terry J and Pianetta P 1992 *Phys. Rev.* B **45** 13 749